Noninvasive high-resolution detection of the arterial and venous input function through a PET Wrist Scanner

A.Kriplani, S.P.Stoll, S. Southekal, D.J.Schlyer, S.J. Park, A. Villanueva J.F.Pratte, S.Junnarkar, P.Vaska, C.L.Woody

Abstract– In order to assess the kinetics of radiotracer accumulation in tissue, the amount of radioactivity in the blood must be quantitatively measured as an input function to the kinetic model. Due to safety and comfort issues with invasive determination of the input function, a non-invasive method for arterial measurement of blood radioactivity is investigated using a wrist scanner. A prototype consisting of two detector pairs of LSO and APD detector arrays is used to obtain planar images of an anatomically correct wrist phantom. The spatial resolution and sensitivity of the prototype is determined. The results showed the detector was able to discriminate the arterial and venous flows from each other when using planar coincidence images.

I. Introduction

Quantitative Positron Emission Tomography (PET) often requires obtaining discrete blood samples which are used to generate an input function for kinetic modeling [1]. The current method for obtaining these blood samples is by placing a catheter in the patient's radial artery [2]. The problems with this method are discomfort to the patient and the risk of medical personnel being exposed to potential blood borne diseases or radioactive contamination while collecting blood samples. Therefore, alternative sampling devices and methods are being considered to help determine the input function. These techniques include external monitors and PET scanners that measure standardized input functions, non-invasively sampled input functions or image derived input functions. Several groups have used standardized input functions (averaged across subjects) or modeled input functions to approximate the actual input function [3]-[6]. However, because the input function can be dependent on individual physiological states and technical variables such as differences in injection rates, these methods can lead to inaccurate parameters for the physiological models. Other groups have used the tomograph itself and examined the possibility of obtaining an input function using large blood vessel imaging [7]-[10]. This approach is limited for several reasons. First, the tomograph has a partial volume effect determined by the spatial resolution and the size of the vessel. Second, an artery large enough to give reliable data may not be in the field of view. Third, the temporal resolution may be determined by the frame acquisition rates specific for a study. Although list mode acquisition capabilities reduce restrictions associated with slower acquisition rates, many scanners do not have this ability. Finally, subject placement within the tomograph may affect the accuracy of the input function. Obtaining reproducible positioning of the body is a difficult technical problem and movement of the subject during the scan will introduce additional errors.

An alternative approach is to place a radioactivity detector directly over a blood vessel or lung [11]-[14]. The primary disadvantage of this approach is the substantial background associated with the surrounding tissue. This background must then be subtracted to obtain the true input function. Since this approach is not based on coincidence counts, gamma rays from the surrounding tissue can significantly interfere with the accuracy of the data. Since the input function is often sampled from the radial artery, a new noninvasive detector, the Arterial Wrist Scanner, is being designed to sample the radial arterial blood of the wrist (Figure 1). The scanner will have four unique properties. It will be independent of the PET scanner, it will be portable, it will distinguish between the artery and the background and it will sample in an area of the body with a minimum of tissue attenuation. The approach taken here was to use a flat bed detector array made from lutetium oxyorthosilicate (LSO) in an array of 4x8 crystals. This detector would create planar images. It has better crystal arrays and light collection than the one previously used [15] along with a small avalanche photodiode (APD) array that closely matches the size and arrangement of the elements in

Manuscript received November 11, 2005. This research was carried out at Brookhaven National Laboratory under contract DE-AC02-98CH10886 with the U.S. Department of Energy as a collaboration between BNL and the State University of New York at Stony Brook.

A. Kriplani is with SUNY @ Stony Brook, Stony Brook, NY USA (telephone: 631-344-4576, e-mail: aarti@bnl.gov).

S. P. Stoll is with Brookhaven National Laboratory, Upton, New York 11973 (telephone: 631-344-5331, e-mail: stoll@lbnl.gov).

S. Southekal is with SUNY @ Stony Brook, Stony Brook, NY USA (telephone: 631-344-4576, e-mail: southekal@bnl.gov).

D. J. Schlyer is with Brookhaven National Laboratory, Upton, New York 11973 (telephone: 631-344-4587, e-mail: schlyer@bnl.gov)

S.J.Park is with Brookhaven National Laboratory, Upton, New York 11973 (telephone: 631-344-4974, e-mail: sjpark@bnl.gov)

A. Villanueva is with Brookhaven National Laboratory, Upton, New York 11973 (telephone: 631-344-4576, e-mail: azaelvillaesp@yahoo.com)

J.F.Pratte is with Brookhaven National Laboratory, Upton, New York 11973 (telephone: 631-344-4986, e-mail: jfpratte@bnl.gov)

S.Junnarkar is with Brookhaven National Laboratory, Upton, New York 11973 (telephone: 631-344-6197, e-mail: sachin@bnl.gov)

P. Vaska is with Brookhaven National Laboratory, Upton, New York 11973 (telephone: 631-344-6228, e-mail: vaska@bnl.gov)

C. L. Woody is with Brookhaven National Laboratory, Upton, New York 11973 (telephone: 631-344-2752, e-mail: woody@bnl.gov)

the crystal block. This technical advancement reduces the size of the radial monitor while at the same time improving the statistics of the gamma detection. Each crystal in the array has the dimensions of 2x2x15 mm3. The crystal array is attached directly to an APD for the conversion of scintillation photons to electronic signals. Pairs of these arrays will be used to count the photons in coincidence over the radial artery in the wrist. These coincidence counts can then be used to quantify the activity and produce an input function of the radiotracer concentration. To test how effective this new device would be in measuring the input function, the signal sensitivity and image resolution were measured using an anatomically correct wrist phantom.

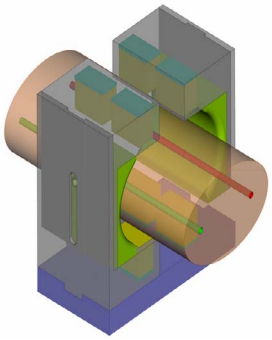

Fig.1. Conceptual design of the wrist detector using 8 detector modules

II. Methodology

A. Materials

A wrist phantom was designed using MRI images of the human wrist in order to have anatomically correct placement of the blood vessels. The wrist phantom was composed of a 63x60.5x48mm Lucite block with two 4 mm diameter holes representing the arteries and two 4 mm holes representing the veins (Figure 2). This phantom was placed between the two pairs of detector arrays, which are ~48mm apart for this prototype. Using this arrangement, it was possible to measure the number of counts arising from both the artery and vein and the possible background noise (or interference) expected from a vein

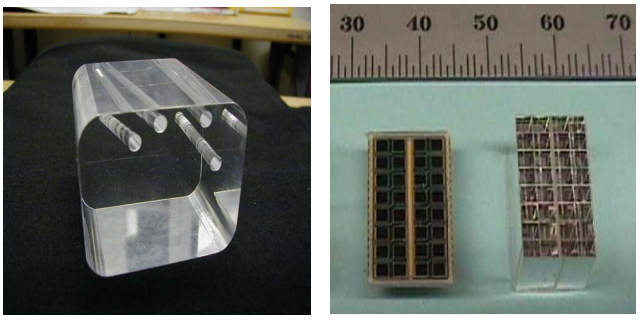

Fig. 2. Left: Picture of the wrist scanner phantom. Right: LSO-APD array used for measurement of input function.

B. Experimental Methods

Preliminary experimental work included a temporal sensitivity measurement which was carried out by placing 2μCi of fluorine-18 in an aqueous solution in the tubing inside the phantom. The flow of fluid would start first from the reservoir of water, then switched to the hot solution and lastly switched back to reservoir of water all in a one-pulse (Figure 3). The flow rate for the experiment was ~7.2 mL/min. Detector counts were accumulated over a seventy second time period. The temporal response of the system was determined to ensure that it would be possible to follow the fast increase and decrease of activity associated with a normal input function.

To determine the attenuation effects of the phantom, an experiment was conducted where the tubing was placed between the two detectors without the Lucite phantom in place. A known concentration of radioactivity (2μCi of $^{18}F^-$) was pumped through the tubing and the number of counts recorded. Subsequently, the tubing was placed in the Lucite block and the block was placed back between the detectors. The same concentration of radioactivity (allowing for radioactive decay) was pumped through the tubing and the number of counts recorded. The ratio between the number of counts per nCi/cc recorded with and without the Lucite block in place gives a measure of the attenuation and scatter inside the block.

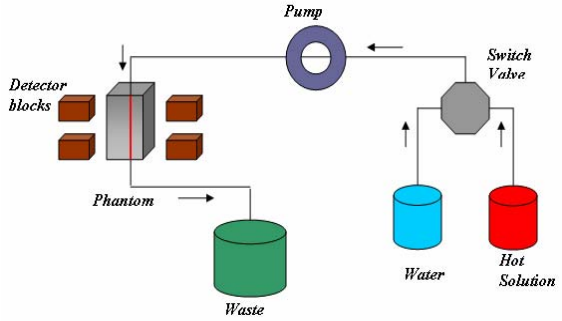

Fig. 3. Experimental setup

A second experiment was performed to determine if there would be interference from the venous blood vessels which are in close proximity to the arteries. The centers of arterial and venous lines are 4mm apart. To estimate the spatial resolution a series of experiments were done with 1 mm diameter Ge-68 rod sources placed in the artery and/or vein channels in the wrist phantom. Using this experimental setup counts were collected for approximately 150 seconds and a high resolution planar image was generated to determine if the artery can be visually separated from the vein. The activity was allowed to decay in place in the tubing to simulate an image with a long acquisition time. The image acquired over a long period of time was then used to identify regions of interest in the wrist.

C. Electronics and Data Acquisition System

Detectors for the wrist scanner are based on Hamamatsu 4 × 8 APD arrays (S8550) coupled to lutetium oxyorthosilicate (LSO) scintillators of 2 × 2 × 15 mm^3. The detectors are coupled to a custom front-end Application-Specified

Integrated Circuit (ASIC), which is a 32 channel device consisting of the preamp, shaper and zero crossing discriminator, and an encoder to generate the 5 bit priority encoded address of the channel that fired. The design was carried out in 0.18 mm CMOS in order to minimize space and power and produces ~ 125 mW per chip (~ 4 mW per channel). The readout circuitry consists of a flexible kapton readout circuit that goes around the wrist connecting all 4 detector blocks (figure 4). These are connected to the associated circuitry for controlling power and communication. In order to minimize the number of interconnections with the Data Acquisition System (DAQ) to optimize the camera's mobility, the 32 channel ASIC has a single output where the timing information of each event and the associated pixel address are serially encoded. The integrated read-out electronic and data acquisition system for this first prototype of the wrist scanner is based on the same architecture of the RatCAP system [16]. Detailed description on the front-end electronic can be found in [17]-[19] and the DAQ in [20] [21]. The data is acquired as individual events each with a time stamp which allows us maximum flexibility in analyzing and using the data.

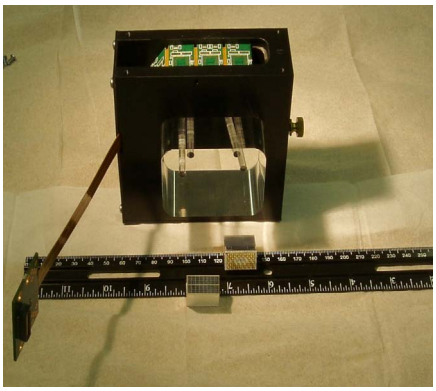

Figure 4: Wrist scanner prototype

A new version of the read-out printed circuit board, dedicated to the wrist scanner which will fit the physiological requirements of a human wrist and the read-out of the eight LSO/APD detector blocks, as seen in Figure1, is currently under development.

III. RESULTS

Figure 5 is a planar image of a Ge-68 rod source inserted into 2 channels of the wrist phantom. The planar image can be used to estimate the sensitivity and the uniformity of the block-detector system. In the image, the radial artery and vein are clearly separated. The image can be used to place regions of interest over the arteries in the wrist that can then be used to generate the time activity curve for the input function

When a solution containing 2 microcuries/cc was passed through the tube representing the artery, an efficiency of 0.2 cps/nCi was obtained. The field of view contains 0.06 cubic centimeters of active volume (2 mm diameter tube by 2 cm length) Figure 6 shows the attenuation of the gammas by the wrist phantom.

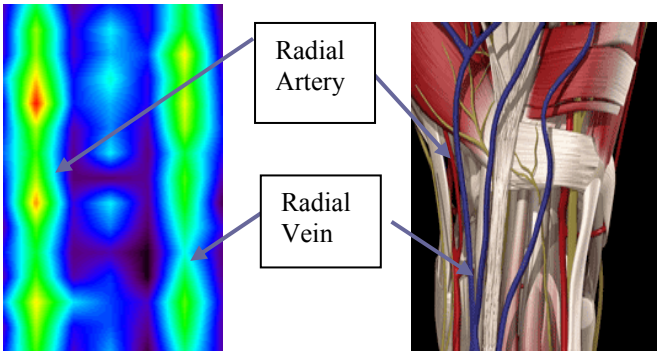

Fig 5. Left: A planar image of the wrist phantom taken with 1 mm diameter Ge-68 rod source placed in the artery and vein channels in the wrist phantom. Right: The anatomical view of these vessels. (Wrist figure taken from http://www.human-anatomy.net/anatomy-wrist pictures.html)

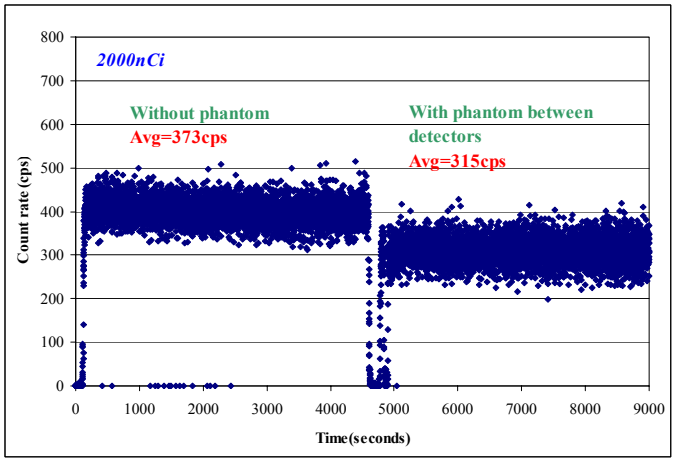

Fig. 6. Attenuation correction measurement of the wrist monitor. The first pulse is a measurement without the lucite wrist phantom in place between the detectors. The second pulse has the wrist phantom between the detectors.

IV. DISCUSSION AND CONCLUSION

The wrist scanner will enable the noninvasive measurement of the input function, thereby eliminating direct arterial sampling. The main concern of such a noninvasive measurement is optimizing spatial resolution while maintaining detection efficiency. Activity in the surrounding veins will produce a significant background which can be rejected using the good spatial resolution of the wrist monitor. The prototype has a sensitivity of 0.2cps/nCi and sufficient spatial resolution to delineate the arterial channel of the phantom from the venous channel.

The high resolution of the detectors combined with the ability to simultaneously measure venous radioactivity and subtract it from the arterial signal, will make it possible to measure the arterial input function. From our previous results[22] using the Lucite wrist phantom, we have found that increasing the crystal length from the 10 mm to the 15 mm increases the sensitivity by more than a factor of two. This comes from the fact that we are in the nearly linear region of the gamma attenuation curve and the sensitivity is increased

by a factor of almost 1.5. Since these are in coincidence we gain a factor of just over 2. Our calculations suggest that eight of these detector modules working in coincidence with focal plane imaging will give us sufficient sensitivity to get an accurate input function. We are currently constructing an 8 detector module array for these tests. The configuration of the detectors on the wrist is shown in Figure 7. The figure shows how the detectors will be placed to maximize the view of the arteries while minimizing the effect of the venous contribution. The other four detectors are placed directly opposite. If the background and randoms from nearby sources decrease our signal to noise ratio, we have the options of increasing the crystal length to 20mm, increasing the number of crystal arrays in the detector to twelve with three along each artery. Going to 12 modules and increasing the length of the crystal to 20 mm will increase the sensitivity by about 2.7 relative to the 8 modules of 15 mm crystals design.

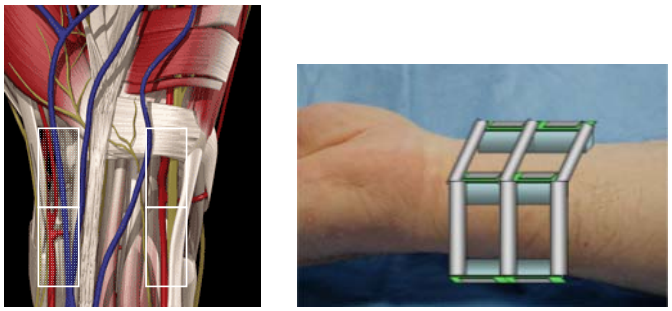

Fig. 7. Left diagram shows the placement of the 8 detector modules (4 on each side) over the radial and ulnar arteries in the wrist. Diagram on the right shows placement of detectors on the wrist.

Focal plane imaging will be used to reconstruct the image to maximize the signal to noise ratio of the arterial image. We can also increase crystal length and perform energy corrections to correct for any cross talk occurring between crystals [23]. To improve and optimize the image quality, we can perform corrections of the focal plane images through normalization measurements and scatter background estimations. Other future design considerations may include external background checks for determining the amount of wrist monitor shielding and tissue background measurements for a quantitative determination of low levels of activity (~200 nCi/cc). Currently simulation studies are in progress. These longitudinal tomographic simulations will explain the geometric effects of changing detector configuration and provide optimal detector spacing.

ACKNOWLEDGMENT

The authors sincerely acknowledge Proteus and CTI, Inc. This research was carried out at Brookhaven National Laboratory under contract DE-AC02-98CH10886 with the U.S. Department of Energy as a collaboration between BNL and the State University of New York at Stony Brook.

REFERENCES

[1] M. E. Phelps, J. Mazziotta, and H. Schelbert, Positron Emission Tomography and Autoradiography: Principles and Applications for the Brain and Heart Raven Press, New York, pp. 287-346, 1986

[2] T. F. Budinger and R. H. Huesman, "Ten precepts for quantitative data acquisition and analysis," *Circulation*, vol. 72, no. 5 Pt 2, pp. 53-62, Nov. 1985.

[3] S. Eberl, A. R. Anayat, R. R. Fulton, P. K. Hooper, and M. J. Fulham, "Evaluation of two population-based input functions for quantitative neurological FDG PET studies, " *Eur. J. Nucl. Med.*, vol. 24, pp. 299-304, 1997.

[4] S. Takikawa, V. Dhawan, P. Spetsieris, W. Robeson, T. Chaly, R. Dahl, D. Margouleff, and D. Eidelberg, "Noninvasive quantitative fluorodeoxyglucose PET studies with an estimated input function derived from a population-based arterial blood curve," *Radiology*, vol. 188, pp. 131-136, 1993.

[5] T. Tsuchida, N. Sadato, Y. Yonekura, S. Nakamura, N. Takahashi, K. Sugimoto, A. Waki, K. Yamamoto, H. Nobushige, and Y. Ishii, "Noninvasive measurement of cerebral metabolic rate of glucose using standardized input function," *J. Nucl. Med.*, vol. 40, pp. 1441-1445, 1999

[6] N. Sadato, Y. Yonekura, M. Senda, Y. Magata, Y. Iwasaki, N. Matoba, T. Tsuchida, N. Tamaki, H. Fukuyama, H. Shibasaki, and J. Konishi, "Noninvasive measurement of regional cerebral blood flow change with $H_2{}^{15}O$ and positron emission tomography using a mechanical injector and a standard arterial input function," *IEEE Trans. Med. Imaging*, vol. 12, pp. 703-710, 1993.

[7] Chen, K, Bandy, D., Reiman, E., Huang, S-C, Lawson, M., Feng, D, Yun, L-S, Palant, A., Noninvasive Quantification of the Cerebral Metabolic Rate for Glucose Using Positron Emission Tomography and 18F-Fluoro-2-Deoxyglucose, the Patlak Method, and an Image-Derived Input Function. J. Cereb. Blood Flow and Metab. 18, 716-723.1998

[8] Ohtake, T., Kosaka, N., Yokoyama, I., Moritan, T., Masuo, M., Iizuka, M., Kozeni, K., Momose, T., Oku, S., Nishikawa, J., Sasaki, Y., and Iio M., Noninvasive Method to Obtain Input Function for Measuring Tissue Glucose Utilization of Thoracic and Abdominal Organs, J. Nucl. Med., 32 1432-1438. 1991

[9] Saabria-Bohorquez SM, Maes A, Dupont P, Bormans G, de Groot T, Coimbra A, Eng W, Laethem T, De Lepeleire I, Gambale J, Vega JM, Burns HD.. Image-derived input function for [^{11}C]flumazenil kinetic analysis in human brain. Mol Imaging Biol. Mar-Apr;5(2):72-8. 2003

[10] Asselin MC, Cunningham VJ, Amano S, Gunn RN, Nahmias C. Parametrically defined cerebral blood vessels as non-invasive blood input functions for brain PET studies. Phys Med Biol. Mar 21;49(6):1033-54. 2004

[11] Nelson, A.D., Miraldi, F., Muzic, R.F., Leisure, G.P., and Semple, W.E. Noninvasive Arterial Monitor for Quantitative Oxygen-15 Water Blood Flow Studies, J. Nucl. Med. 34:1000-1006. 1993

[12] H. Watabe, M. Miyake, Y. Narita, T. Nakamura, M. Itoh, Development of Skin Surface Radiation detector system to monitor radioactivity in arterial blood along with Positron Emission Tomography, IEEE Trans Nucl Sci. 42(4) 1455-1459. 1995

[13] M. Aykac, R.D. Hichwa , G.L. Watkins. Investigation of a noninvasive detector system for Quantitative [O-15] water Blood Flow Studies in PET. IEEE Transactions on Nuclear Science, VOL. 48(1) Feb. 31-37. 2001

[14] Yamamoto, S.; Matsuda, T.; Hashikawa, K.; Nishimura, T. Imaging of an artery from skin surface using beta camera IEEE Transactions on Nuclear Science, Volume: 46(3) 583 – 586. 1999

[15] Rajeswaran, S. Baily, D.L. Hume, S. P Townsend, D.W.. Geissbuehler, A Young, J..Jones, T. 2-D and 3-D imaging of small animals and the human radial artery with a high resolution detector for PET. IEEE Transactions on medical imaging, 11(3):385-391. 1992

[16] Vaska, P.; et. al.; "RatCAP: miniaturized head-mounted PET for conscious rodent brain imaging" IEEE Trans. Nucl. Sci vol. 51, no. 5, pp.2718 – 2722, Oct. 2004

[17] Front-end electronics for the RatCAP mobile animal PET scanner: timing discriminator and 32 line address priority serial encoder Pratte, J.-F., Junnarkar, S., O'Connor, P., Woody, C., Stoll, S., Villanueva, A., Kandasamy, A., Radeka, V., Bo Yu, Robert, S., Lecomte, R., Fontaine,

R. IEEE Nuclear Science Symposium Conference Record, Rome (Italy), Vol. 4, pp. 2211-15 2004

[18] Design and performance of 0.18-um CMOS charge preamplifiers for APD-based PET scanners Pratte, J.-F., Robert, S., De Geronimo, G., O'Connor, P., Stoll, S., Pepin, C.M., Fontaine, R., Lecomte, R. IEEE Transactions on Nuclear Science, Vol. 51, Is. 5, pp. 1979-85 2004

[19] Front-end electronics for the RatCAP mobile animal PET scanner Pratte, J.-F., De Geronimo, G., Junnarkar, S., O'Connor, P., Bo Yu, Robert, S., Radeka, V., Woody, C., Stoll, S., Vaska, P., Kandasamy, A., Lecomte, R., Fontaine, R. IEEE Transactions on Nuclear Science, Vol. 51, Is. 4, pp. 1318-23 2004

[20] S Junnarkar, M Purschke, J.F. Pratte, S.J.Park, P. O'Connor and R.Fontaine All digital approach to front end signal processing for the mobile animal PET scanner. IEEE Nuclear Science Symposium Conference Record. Puerto Rico. *In press* 2005

[21] M. L. Purschke, A. Kandasamy, P. O'Connor, S.J. Park, J.-F. Pratte, D. J. Schlyer, S. P. Stoll, P. Vaska, A. Villanueva,C. L. Woody, S. Junnarkar, S.Krishnamoorthy, S. Southekal "The Data Acquisition System of the RatCAP Conscious Small Animal PET Tomograph" IEEE Nuclear Science Symposium Conference Record,, Puerto Rico. *In press* 2005

[22] Villanueva, A.., Stoll, S.P. Schlyer, D.J., Shokouhi, S. Vaska, P. Woody, C.L., Kriplani, A. and Volkow, N. 2003. Spatial Resolution of A Noninvasive Measurement Of The Arterial And Venous Input Function Using A Wrist Monitor, Nuclear Science Symposium Conference Record, IEEE. 2232 - 2236. 2003

[23] P. Vaska, S. P. Stoll, C. L. Woody, D. J. Schlyer, and S. Shokouhi, 2003. Effects of Inter-Crystal Cross-Talk on Multi-Element LSO/APD PET Detectors, IEEE Transactions on Nuclear Science, vol. 50(3) 362-366.